Modeling and Simulation of a High-Head Pumped Hydro System

A Thesis

Presented in Partial Fulfillment for the Requirements for the

Degree of Master of Science

with a

Major in Electrical Engineering

in the

College of Graduate Studies

University of Idaho

by

Hang Li

December 2014

Major Professor: Brian K. Johnson, Ph.D

AUTHORIZATION TO SUBMIT THESIS

This thesis of Hang Li, submitted for the degree of Master of Science with a Major in Electrical Engineering and titled "Modeling and Simulation of a High-Head Pumped Hydro System" has been reviewed in final form. Permission, as indicated by the signatures and dates below, is now granted to submit final copies to the College of Graduate Studies for approval.

Major Professor:	_____	**Date:**	_____
	Brian K. Johnson, Ph.D.		
Committee Members:	_____	**Date:**	_____
	Joseph D. Law, Ph.D.		
	_____	**Date:**	_____
	Donald Elger, Ph.D.		
Department Administrator:	_____	**Date:**	_____
	Fred Barlow, III, Ph.D.		
Discipline's College Dean:	_____	**Date:**	_____
	Larry Stauffer, Ph.D.		

Final Approval and Acceptance

Dean of the College of Graduate Studies:	_____	**Date:**	_____
	Jie Chen, Ph.D		

ABSTRACT

High levels of intermittent renewable generation penetration, such as solar or wind, could lead to deviation of the power grid frequency from normal due to the randomness of the output of some renewable energy sources. Conventional peak load plants, i.e. gas turbine plants, lack of the ratings to stabilize the frequency, thus, grid storage is an option to provide extra load balance for renewable energy resources. Pumped hydroelectric storage is an excellent choice due to its low cost, acceptable efficiency, and reliability. This thesis develops models for a feasibility study of a proposed project to utilize a pumped hydro storage system to regulate the frequency of the power grid to meet the North American Electric Reliability Corporation Control Performance Standard Requirement 2 (NERC CPS2) in response to variable renewable energy output. The pumped hydro system should be able to vary the energy input and output to regulate the frequency within each 10 minute interval during its operation. To study this scenario, a dynamic model for the electrical and hydraulic systems is developed and tested using the MATLAB Script function. Simulations studies are performed using randomly generated variable wind generation output to test CPS2 compliance over period of 48 months. The simulation model is able to provide frequency regulation ability to the power grid to meet the CPS2 standard.

ACKNOWLEDGMENTS

I cannot find words to express my gratitude to Dr. Brian Johnson for the continually and persistent help in regard to research and scholarship during my graduate program. I would like to thank my committee members Dr. Joseph Law and Dr. Donald Elger for their guidance and support with their wealthy knowledge in the field of study and making the processes of completing the this thesis enlightening. In addition I would like to thank Greg Parker and Kyle Morse for their essential contribution to this project, it has been pleasure to work in a team with you all. I thank the Department of Electrical and Computer Engineering has been really supportive and made my studying experience enjoyable. I really appreciate all the assistance from everyone which made my achievement possible. I would also like to thank my parents for always believing in me and supporting me. I could not have achieve this far without my parents support.

TABLE OF CONTENTS

LIST OF FIGURES

LIST OF TABLES

CHAPTER I. INTRODUCTION

I - A. MOTIVATION

Renewable energy sources are receiving increased attention because they are sustainable; all renewable energy (except tidal and geothermal power), and even the energy in fossil fuels, ultimately comes from the sun. The sun radiates $174{,}423{,}000{,}000{,}000$ kilowatt hours of energy to the earth per hour. In other words, at any moment, the earth receives 1.74×10^{17} watts of power. About 1 to 2 per cent of the energy coming from the sun is converted into wind energy [1]. That is roughly $2 - 3 \times 10^{15} Watt$ of available wind energy worldwide. The world energy consumption in 2013 was 697 Mtoe (million tonne of oil equivalent) [2] and that converts to 9.25×10^{11} watts of power. Therefore, the potential wind energy is several magnitudes larger than the world's energy demand.

Wind and solar power worldwide have become the fastest growing renewable energy sources in the past few years. As shown in Figure 1, renewable energy sources, excluding hydro power, are growing at a mean annual rate of 15.1%; the renewable electricity share, ignoring hydropower, has picked up 3 percentage points in its share of global electricity production, rising from 1.6% of the total in 2002 to 4.6% in 2012 [3].

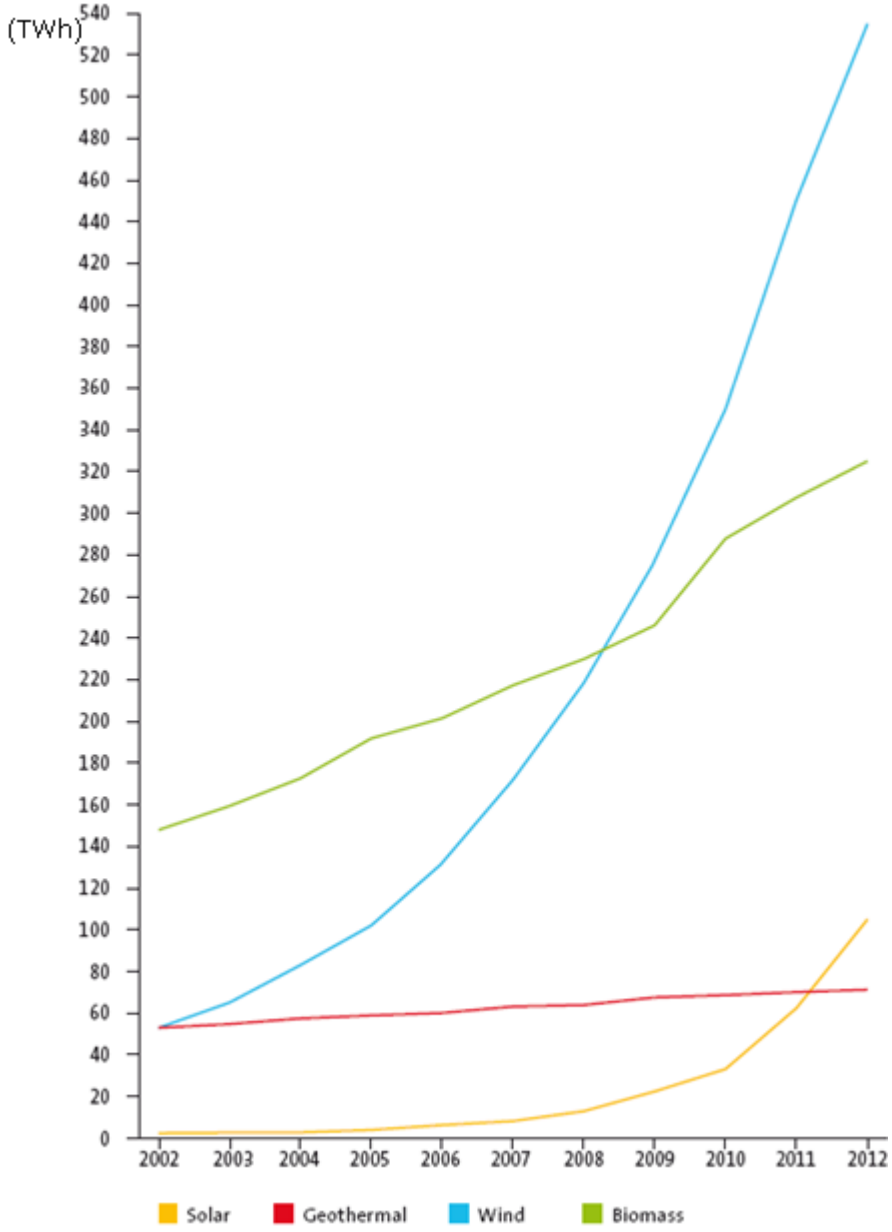

Figure 1 Renewably-Sourced Electricity Production, Excluding Hydraulic (TWh) [3]

However, the amount of energy generated by solar and wind generation can vary randomly, and usually the generated power does not match the power demand. Figure 2 [4] shows the load mismatch created by high variations in wind generation which can potentially make the grid unstable as the penetration continues to increase. As long as the majority of the generators are synchronous machines, when the total generated

power exceeds the total load power, the frequency of the grid will increase and the frequency will decrease when the load is greater than the generated power. The penetration of intermittent renewable energy in the grid is limited to a small portion of the total generated power due to several barriers [5], one of which is frequency deviation.

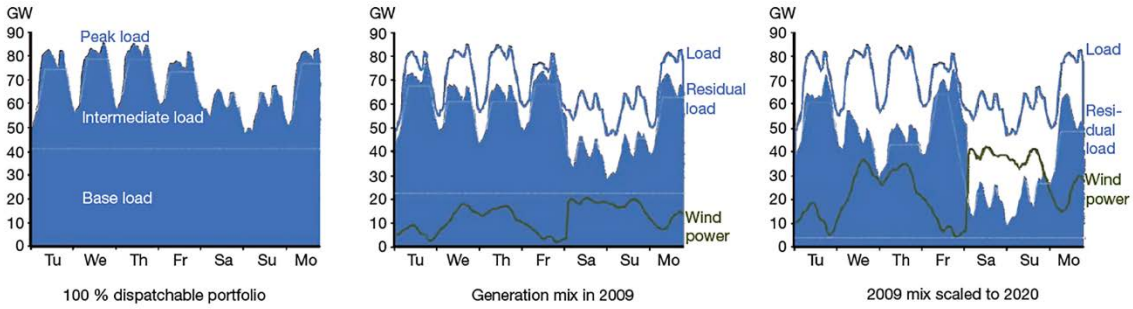

Figure 2 Load Mismatch due to Increased Wind Penetration [4]

I - B. OBJECTIVE OF THE WORK

The objective is to model a pumped hydro system to compensate renewable sources to stabilize the grid frequency to meet the North American Electric Reliability Corporation (NERC) reliability standards [6] for electric energy markets. The Control Performance Standard Requirement 2 (CPS2) [7] is the standard used for frequency regulation. The CPS2 will be discussed in detail in II - A.

This thesis will present a pumped storage simulation model implemented using MATLAB. The model will incorporate electric machine dynamics as well as hydraulic dynamics. The resulting simulation models are used in a feasibility study for the ability of a pumped storage system to regulate frequency to meet the NERC CPS2 in response to variable renewable energy output.

I - C. THESIS ORGANIZATION

This thesis is organized and documented to cover the research accomplished during a research project. Section Chapter II provides the background of the pumped storage technologies including the advantages and disadvantages of currently in service pumped storage sites for general grid needs and for meeting the CPS2 requirement. Chapter III contains an overview of the pumped storage system that is to be modeled. Chapter IV describes both the electrical and hydraulic components used in the simulation. Chapter V provides a simulation example demonstrating performance of the pumped hydro storage model with variable generation on the power system. Simulation results are presented and analyzed. Section Chapter VI includes summaries, conclusions, and describes potential future work.

CHAPTER II. BACKGROUND

II - A.NORTH AMERICAN ELECTRIC RELIABILITY CORPORATION (NERC) CPS2

The NERC CPS2 sets the limit for the mismatch, described as area control error, between generation and load. It states that a non-violation month has an average area control error less than a specified limit for at least 90% of ten-minute time periods during that calendar month. CPS2 compliance is achieved if more than 90% of the ten-minute intervals satisfy the mismatch limit in a calendar month.

Balancing authorities are required to provide regulation to meet the NERC reliability standards. A typical balancing authority is a utility power operating center. There are over 100 Balancing Authorities of varying size in North America. Each Balancing Authority in a local interconnection is connected via high voltage transmission lines (called tie-lines) to neighboring Balancing Authorities [8]. Within the balancing authority's system, load or variable energy resources may be changing during any time period. The balancing authority must adjust its dispatchable resources to compensate for the changes in load or variable generation. The adjustment is known as regulation. Ultimately, maintaining system frequency within some desirable tolerance is a higher priority than matching a generation schedule.

The area control error is determined by:

$$ACE = (NI_A - NI_S) - 10 \cdot B_s \cdot (F_A - F_S) - I_{Me} \quad (1)$$

Where:

NI_A Actual power flow

NI_s Scheduled power flow

B_s Frequency bias setting $(MW/0.1Hz)$

F_A Actual frequency

F_S Scheduled frequency, typically $60Hz$

I_{ME} Meter error correction factor (small or zero)

The metric for CPS2 is determined by the following:

$$L_{10} = 1.65\epsilon_{10}\sqrt{(-10\beta_i)(-10\beta_s)} \quad (2)$$

Where:

L_{10} in MW is the metric for CPS2

ϵ_{10} in Hz is the frequency deviation bound determined for each interconnection

β_i in $MW/0.1Hz$ is the frequency bias. It shall be assumed to be 1% of the variable generation capacity, in the case of wind generation.

β_s in MW/0.1Hz is the sum of the frequency bias with in an interconnection.

The following is an example calculating the L_{10} boundary for a $1200MW$ wind farm within an interconnection. The L_{10} sets the limit of mismatch of each ten-minute interval.

$\epsilon_{10} = 0.0073Hz$

$B_s = -2000MW/dHz$

$B_i = -0.1 \cdot 1200MW = -12MW/dHz$

$L_{10} = 1.65 \cdot 0.0073Hz \cdot \sqrt{(-10 \cdot -2000MW/dHz)(-10 \cdot -12MW/dHz)}$

$\boxed{L_{10} = 18.66MW}$

$NI_A = 1150MW$

$NI_S = 1000MW$

$\boxed{NI_A - NI_s = 150MW}$

$B_s = 2000MW/0.1Hz$

$F_A = 59.927Hz(-0.0073Hz)$

$F_S = 60Hz$

$I_{ME} = 0$

$ACE = 1150MW - 1000MW - 10 \cdot 2000MW/0.1Hz \cdot (59.927Hz - 60Hz)$

$- 0$

$\boxed{ACE = 4MW}$

In the example the balancing authority generated more power than was scheduled based on $NI_A - NI_s$, however the interconnection had an under frequency situation based on F_A. Ultimately the goal of the BA is to maintain the grid frequency rather than matching the schedule, therefore, the calculated area control error is only 4 MW; well under the 18.66 MW limit. As a result there is no violation for that 10min period.

II - B.ADVANTAGES OF PUMPED STORAGE FOR AVOIDING CPS2 VIOLATIONS

In order to achieve higher renewable energy penetration without the grid becoming unstable, dynamic energy compensation is needed. Energy storage can "smooth" the delivery of power generated from wind and solar technologies, in effect, increasing the value of renewable power [9]. Traditionally, intermediate plants and peak plants are used as dispatchable resources to match the generation and the load. Those plants are often powered by natural gas, but they can also be powered by water at hydroelectric dams or by fuel oil [10]. However, there is limited capacity to smooth load as generation varies; conventional gas and coal generators cannot operate continuously at low power output, and they take a few minutes to start and connect synchronously to the grid [11] and are not as effective for providing compensation. Therefore, a fast responding energy storage system needs to be implemented for real time compensation. Common energy storage methods are: batteries, pumped hydro storage plants (PSP), compressed air energy storage (CAES), and hydrogen electrolysis [4]. Each of the methods has its own advantages and disadvantages. However, round trip storage

efficiency is one of the most important aspects when it comes to performance measures. Table 1 shows the efficiency comparison between different storage methods. The technologies listed on the table are: lithium ion batteries (Li-ion), lead acid batteries (lead-acid), pumped storage plant (PSP), vanadium redox flow batteries (VRB), nickel cadmium and nickel metal hydride batteries (NiCd, NiMh), advanced adiabatic compressed air energy storage (AA-CAES), compressed air energy storage (CAES), and hydrogen electrolysis (Hydrogen).

Technology	Cycle efficiency
Li-ion	90 – 95 %
Lead-acid	80 – 90 %
PSP	75 – 80 %
VRB	~75 %
NiCd, Ni-metal hydride	70 %
AA-CAES	< 70 %
CAES	42 – 54 %
Hydrogen*	<40 %

* electrolysis 65 %, compression 97 %, gas turbine combined cycle 60 %

Table 1 Cycle efficiency of various storage technologies [4]

The pumped storage plants have a closed cycle efficiency of $75\% - 80\%$ which means for every $1\ kW \cdot h$ of energy stored, $0.75\ kW \cdot h$ of energy can be put back into the grid. The efficiency of the pumped storage plants is not the highest among the storage methods listed; they are surpassed by the lithium ion batteries and the lead-acid batteries. However when factoring in cost as a factor for large amounts of energy storage, the pumped storage plants have a definite advantage. Figure 3 [4] shows the cost comparison between different storage methods per kilowatt hour.

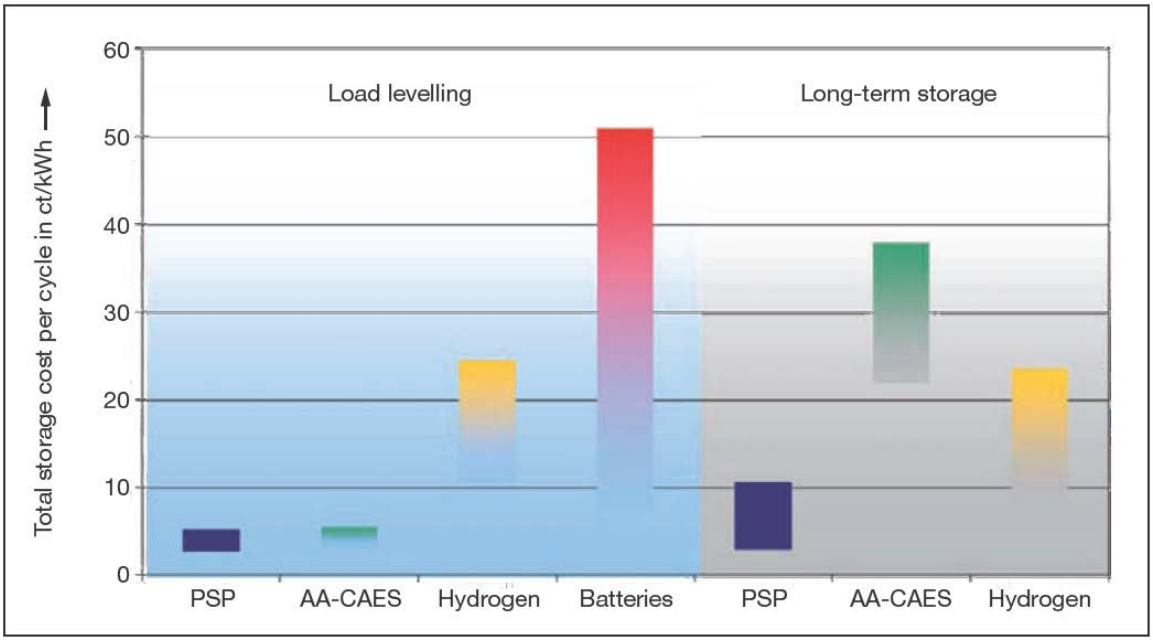

Figure 3 Energy storage costs [4]

It is clear that pumped hydro storage has the lowest cost per cycle in both load leveling and long-term storage applications; it only costs a fraction of the batteries.

II - C.PUMPED HYDRO PLANTS AND THEIR FUNCTIONALITY

Pumped storage had its beginning in Germany where the first plant was constructed in 1908 [12]. The majority of the pumped storage plants in the U.S. were built from the 1960s to the late 1980s to compensate for fixed output nuclear energy. Fewer facilities were developed during the 1990s; due to saturation of the best available locations and a decline in growth in nuclear development [13]. Figure 4 [12] shows the chronological plot of pumped hydro installed in the United States from 1950 to 1990. Traditionally, pumped storage plants were used to regulate the nuclear energy output over a 24 hour period because nuclear output cannot be varied easily and runs best at constant output power.

Large growth in new renewable energy penetration is demanding massive energy storage to balance variable output, and the pumped hydro plants are in demand for bulk energy storage in utility grids; there are approximately 100 GW in service around the globe and 20 GW operating in the United States as of 2009 [14].

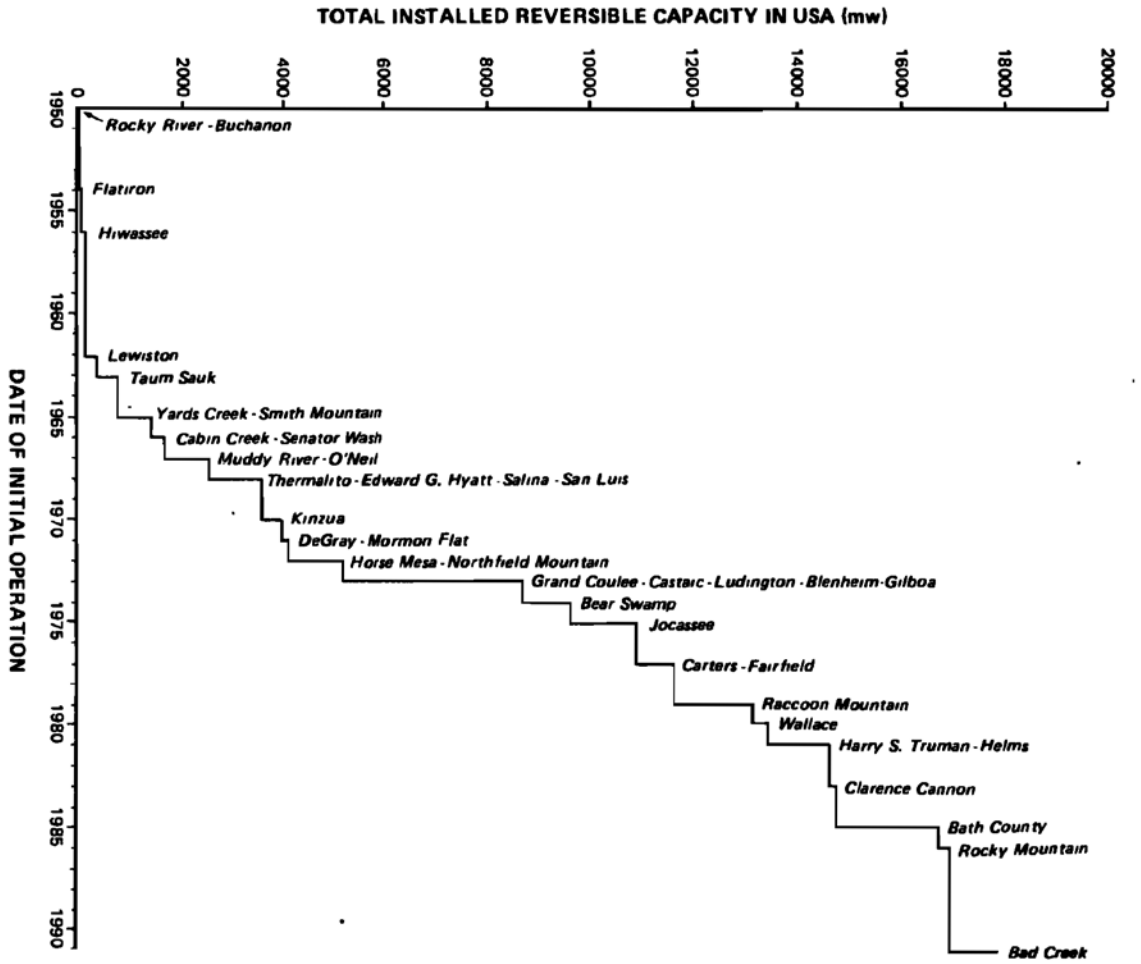

Figure 4 Total Installed reversible capacity in U.S.A hydroelectric pumped storage facilities [12]

The use of pumped hydro storage plants can improve system-wide efficiency and reliability by allowing system operators to time-shift power generated during periods of low demand for electricity for use during high-demand periods [15] as shown in Figure 5 [15].

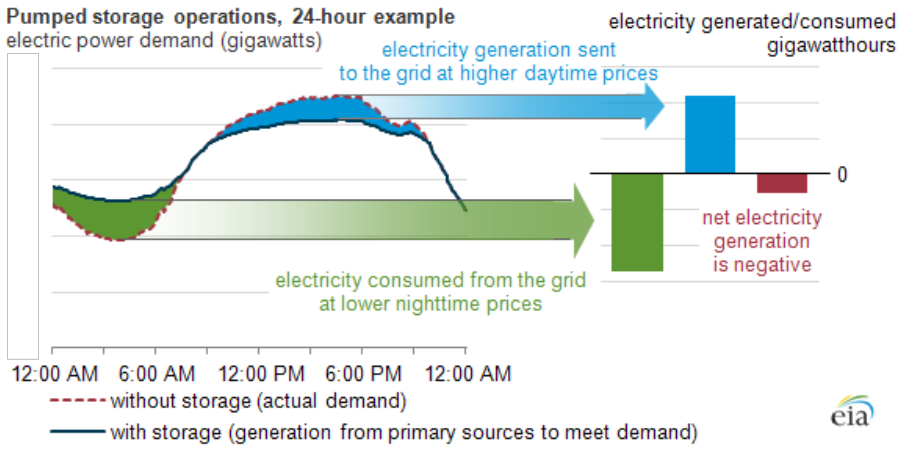

Figure 5 Pumped Hydro Storage Operation for Load Shifting [15]

Additional pumped hydro plants have been proposed and a few are under construction due to the penetration of renewable energy sources. When pumped hydro storage plants are used for load shifting they typically consume electricity during low-demand hours (e.g., nighttime) and put power back on the grid when electricity demand is high (daytime) [15]. The frequency of reversal from pumping to generating is limited largely due to thermal stress on pump motor with pump motor starts limited to a few times a day. However when the pumped storage is being used for frequency balancing to meet the CPS2 standard described in II - A, the plant needs to cycle between pumping and generating a lot more frequently in order to provide frequency balancing ability, which poses a challenge for the existed pumped hydro plants designed for load leveling. Plants build for frequency balancing need to take the thermal stress put on the electric machine for frequent start and stop operation in account; an ability that load leveling plants don't have. Electric machinery starting and variable speed operation, another capability useful for renewable balancing, will not be included in this stage of the project. However, some research has been done on the topic including the suggestion of

using a doubly-fed induction machines [16] to provide variable speed operation of the pumped hydro plant.

CHAPTER III. GENERAL DESCRIPTION OF PUMPED HYDRO PHYSICAL SYSTEM

Figure 6 shows a simple sketch representing the physical design of the proposed pumped hydro storage system to provide energy balancing ability to the grid.

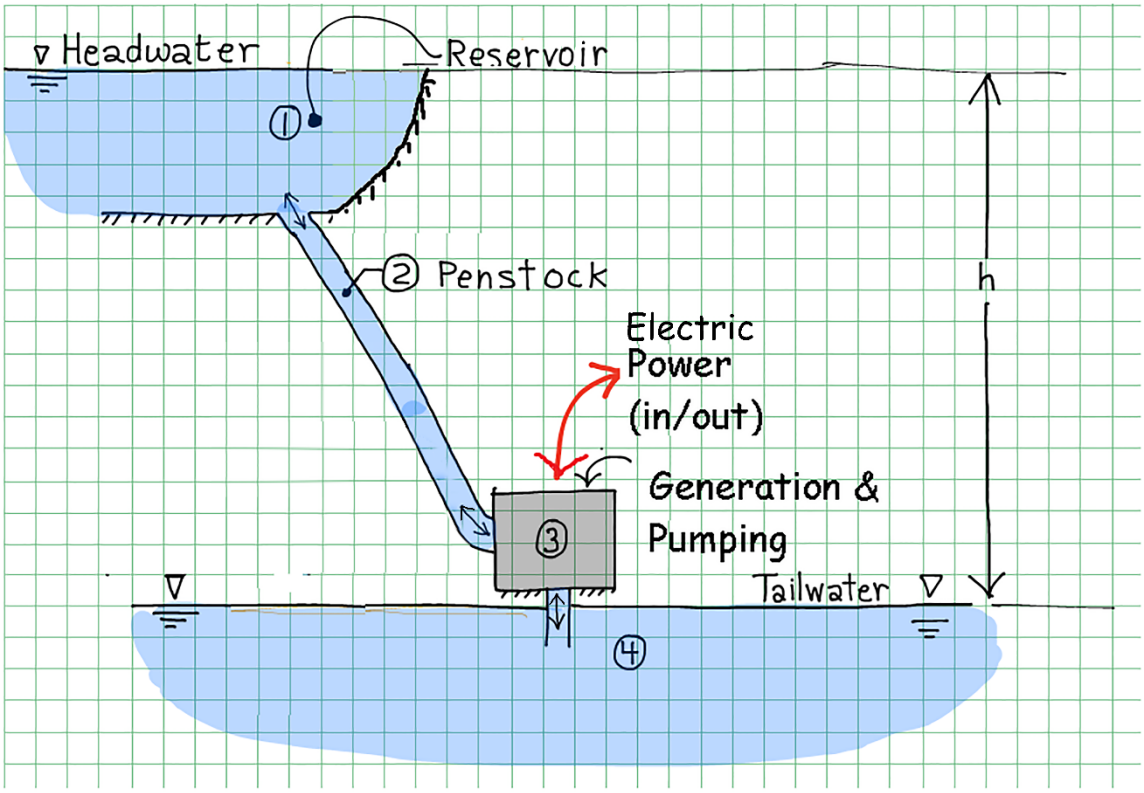

Figure 6 Physical System Layout

During the operation of the pumped hydro plant energy is stored in the upper reservoir in the form of potential energy associated with the increased elevation of the water in the reservoir relative to the elevation of the tail water in ①. When the system is generating power, water flows down the penstock labeled ②. The water flows back up the same penstock during pumping operation; only one penstock is used to simplify the pump storage system design as well as cut down penstock cost. Electric machinery coupled with turbine through a mechanical shaft is located in ③ at the bottom of the

penstock for generation and pumping. The tail water ④ can be a lake or river at a lower elevation.

The diagram in Figure 7 is an illustration of the components of the proposed pumped hydro system along with a simplified external power system.

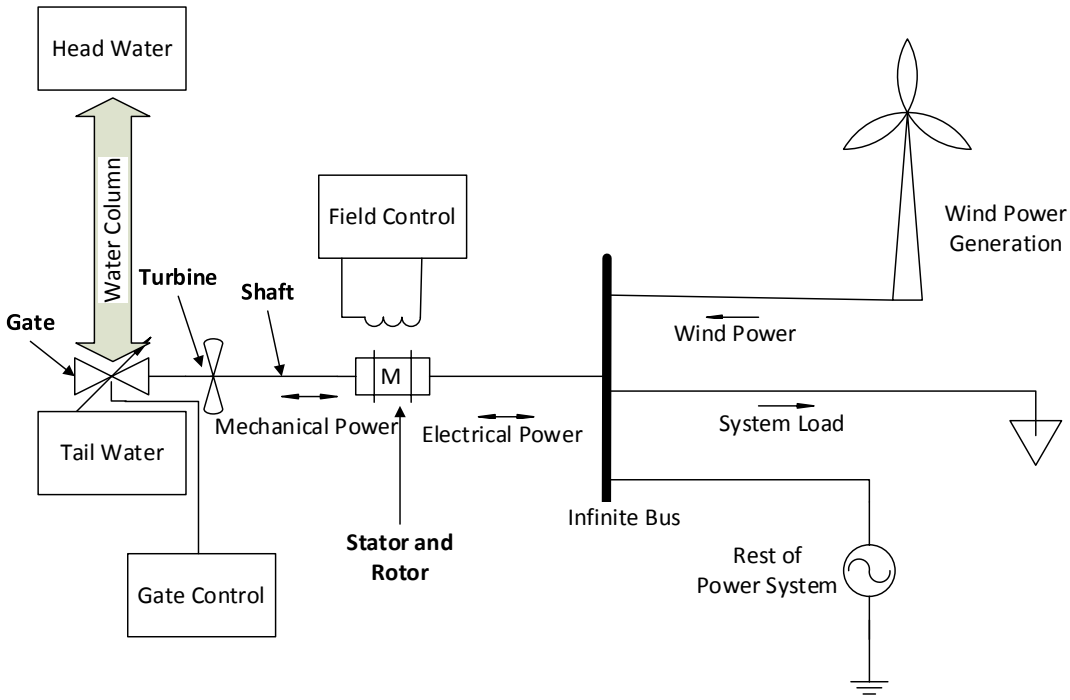

Figure 7 Diagram of simulation system

In the diagram, the gate is the device that controls the water flow and it will directly interact with water column in the penstock. The gate control regulates the rate of opening and closing to limit changes in energy flow to be 2.5%/s. When generating, the turbine harvests the mechanical power from the water flow and delivers the power to the electrical machinery through the shaft, and reverses the process during pumping. The head water is modeled as a body of water with a set maximum water storage capacity and the tail water is considered to be an infinite water supply. The electrical power is transferred between the electric machinery and the point of coupling. Ideally

the net summation of wind power + system load + electrical power from pumped hydro plant is zero. However due to the transient time constant difference between the wind generation, the pumped hydro plant, and the load power, slight power mismatch will happen. To determine if the mismatch stays within frequency control limit, the CPS2 score needs to be calculated. The process of calculating the CPS2 score is shown in Figure 8. The CPS2 Calculation block is described in detail in previous Chapter II - A.

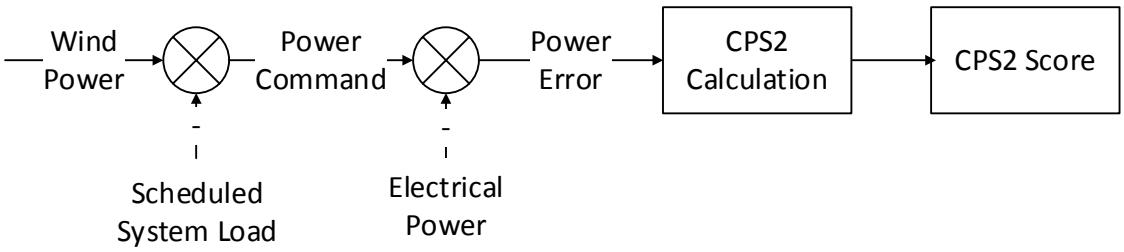

Figure 8 CPS2 calculation process for pumped hydro plant

The power command is calculated from the difference between the wind power generation and the system load power. The power command can be positive, negative, or zero depending on the relationship between the wind generation and the load, i.e. when the wind generation is greater than the system load the power command is positive indicating the pumped hydro plants need to start pumping. When the wind generation is less than the load, the power command will be negative and the pumped hydro plants will be generating. The power command will be zero if wind generation is zero or rest of the power system is able to match the load and wind generation. The power error, which is the mismatch between the power command and the actual pumped hydro power, will be used to calculate the final CPS2 score. The power system

frequency will be taken into account for during the final calculation to provide more accurate pumped hydro plant performance estimation.

The simulation model contains a set of MALTAB scripts that define physical parameters as well as equations governing the transient responses of the components. The flowchart of the dynamic model is shown in Figure 9.

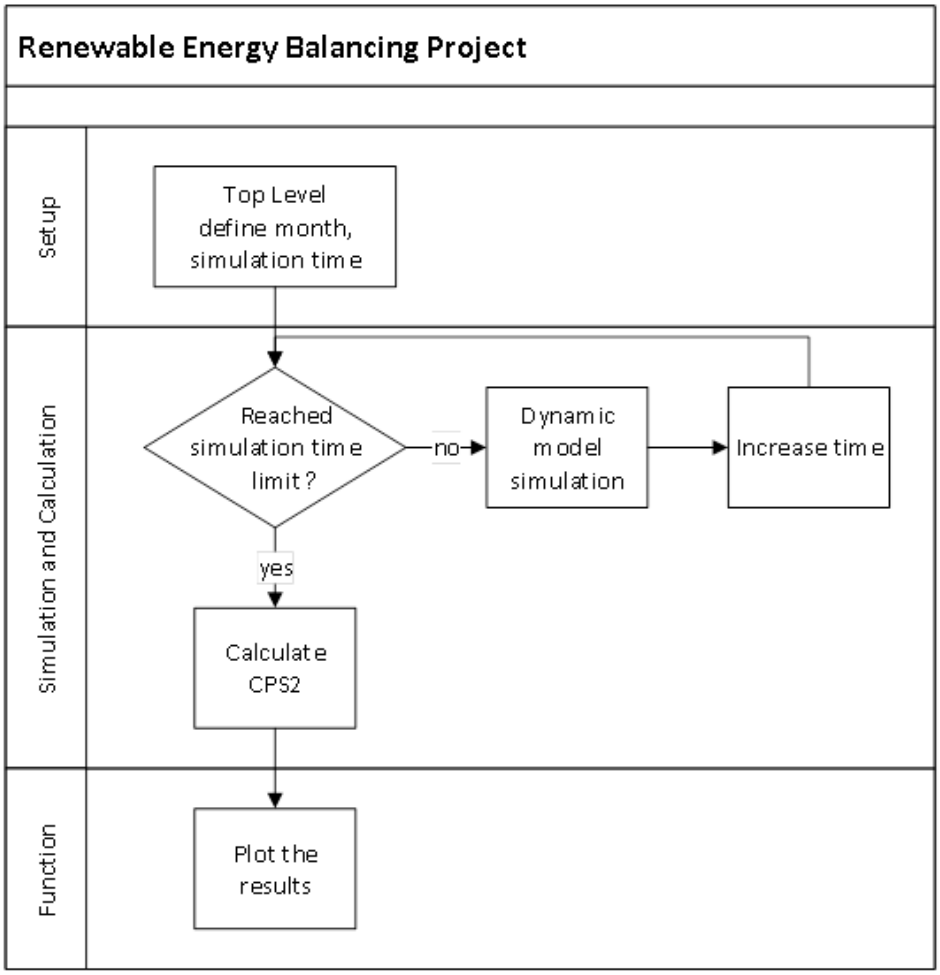

Figure 9 Pumped hydro dynamic model flowchart

In the beginning of the simulation the user defines the simulation time span and the parameters for the pumped storage generation system in the top level, these parameters include which includes penstock dimensions, turbine and gate size, machine

parameters, and length of month. The wind generation data and the load demand data can be either randomly generated within the MATLAB model, provided by another program, or they can be read in from a historical data file. The rate of change of the input and output for pumping and generation is limited to $2.5\ \%/s$, provided in the project specification, in order to reduce the transient water hammer and cavitation effects to help keep the cost of penstock lower. The phenomenon of water hammer may occur in case of sudden change in the velocity of flow in a conduit [17] resulting in a pressure spike in the enclosed pipe. If a more rapid change is desired, a stronger penstock needs to be constructed to sustain the water hammer, which will increase the cost of construction.

The operational time scope for the simulation model of the project is initially set to be a few seconds to a few months which is targeted to cover both transient stability and long term operation stability analysis. Table 2 lists the typical duration responses of events during typical pumped hydro storage plant operation.

Electric machine subtransient (T_d'')	0.01 s – 0.05 s
Electric machine transient (T_d')	1.5 s – 9 s
Gate operation ($2.5\%/s$)	40 s
Load mismatch calculation interval	5 min
CPS2 Score calculation interval	10 min
Pumped hydro long term operation	Weeks

Table 2 Time response of major subsystem under pumped hydro operation

The desired few seconds time span falls during the electric machinery transient response as well as the hydraulic transient response to gate operation. So the desired model needs to represent this behavior. While the long term simulation ranging to months will determine the pumped hydro system self-sustainability to ensure that the pumped hydro plant is able to operate a prolonged period of time without running out of water. The subtransient time period is not going to be needed in this study because the response time is shorter than the minimum period of interest and it would not be numerically efficient to include subtransient for simulation designed to cover time span of a few month; a separate subtransient model that covers shorter time span needs be developed separately to study the subtransient effect on the electric system and the hydraulic system for a more accurate evaluation of stresses caused by these transients. These can be short simulations, not covering hours or weeks or years.

CHAPTER IV. MODELING OF THE ELECTRIC MACHINERY AND PENSTOCK

The electrical system contains the electrical machinery and the power grid. In this case the power grid is treated as a constant voltage source and the machine transient response will be modeled in detail. The hydraulic system contains the penstock, the gate, and the turbine which will also be modeled with a full transient model. A MATLAB Script will be used for instead of Simulink due to its calculation efficiency for long term simulation and expandability for future follow-on projects. The electric machinery is coupled with mechanical components such as the turbine, the gate, and the penstock which will be the source and the sink for the mechanical power. It is crucial to analyze how the pumped hydro storage system reacts to transients in order to generate the most economical design specifications for the components.

The electrical machinery parameters along with other components' rated parameters are defined by the user at the start of the simulation. Those data will be stored in a separate m-file script. The script containing the user defined data will be called by the main MATLAB script for calculation. All the components will be initialized during the first iteration to calculate the initial conditions; those steady state outputs will be used for initial values. The machine startup behavior will not be analyzed in this thesis. The flowchart of the dynamic model is shown in Figure 10.

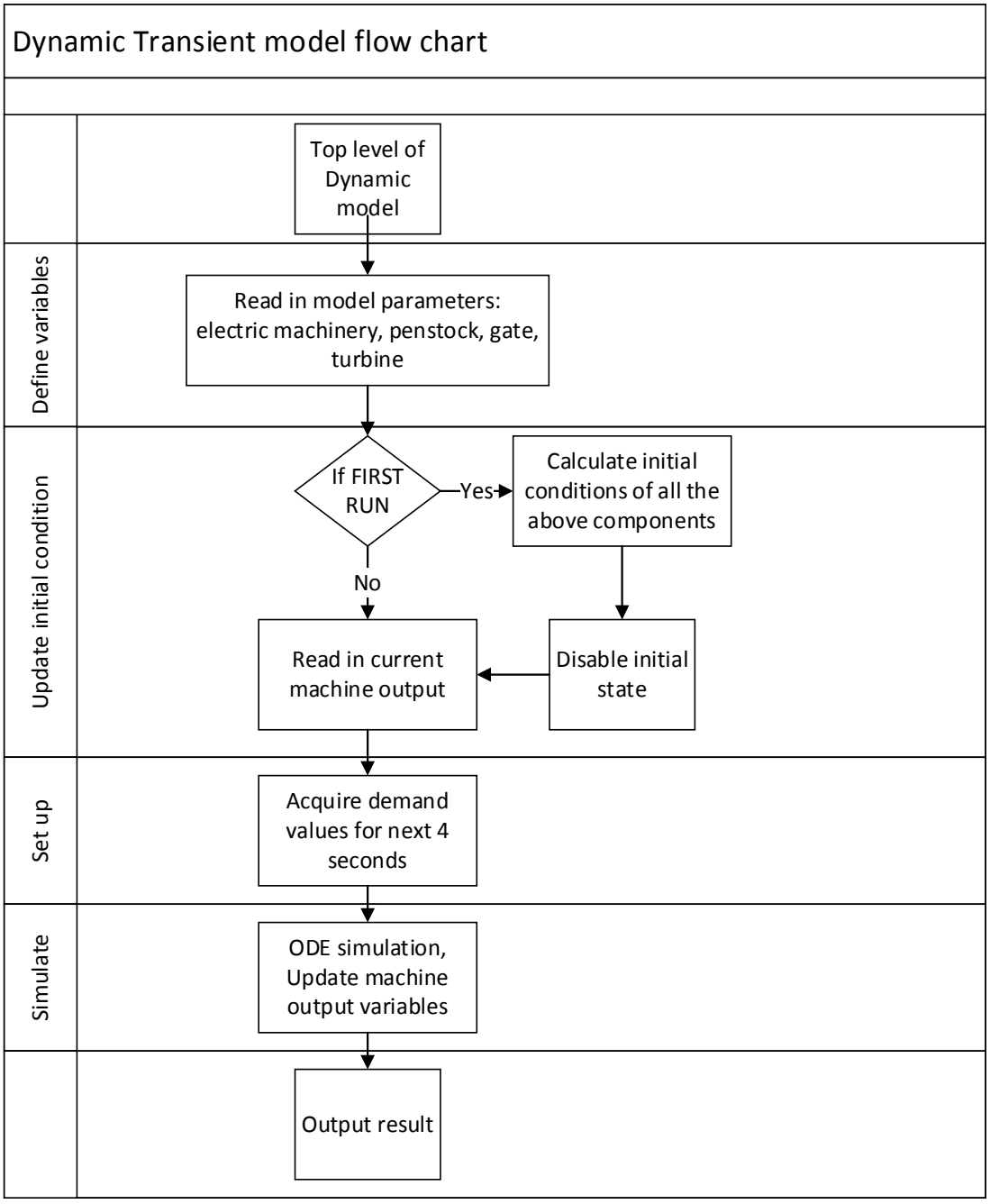

Figure 10 Dynamic generator model flow chart

The model is set up such that both electrical system and hydraulic system initial state will be calculated in the beginning of each simulation run. After the initial conditions are established, all the parameters will be passed onto dynamic model for simulation. The dynamic model uses the MATLAB Ordinary Differential Equation (OED)

solver to solve for components' state for a given four-second period. The last iteration of the previous four second will be saved as the initial state for the next four seconds until the simulation time cap is reached. The time step is determined by the MATLAB ODE solver automatically for optimal performance.

IV - A. ELECTRIC MACHINERY AND HYDRAULIC INITIAL CONDITIONS

IV - A - 1. ELECTRIC MACHINERY INITIAL CONDITIONS

The initial conditions will be calculated during the first iteration of the simulation. Since the actual machine start up is not going to be studied in this stage of the project, the initial conditions are steady state operation of the pumped hydro system at a low generating output of 5% of rated generation power. Equation (3) to Equation (15) are used to calculate the electric machinery initial conditions. All variables are in per unit unless otherwise stated. The equations are defined in the rotating reference frame (dq0 transformation) because under balanced steady – state conditions the transformation eliminates the time varying sinusoidal components from the signal making modeling and analyzing the ac circuit easier [18].

First find the machine internal voltage from terminal voltage and current:

$$E_{x0} = V_{a0} + \left(R_a + i \cdot X_q\right) \cdot I_{a0} \tag{3}$$

$$\theta_{r0} = angle(E_{x0}) - \pi/2 \tag{4}$$

For balanced steady – state conditions, the phase current using the dq0 transformation may be written as follows:

$$I_{a0} = conj(S_{set}/V_{a0}) \tag{5}$$

$$I_{dq0} = I_{a0} \cdot e^{-i \cdot \theta_{r0}} \tag{6}$$

$$I_{ds0} = real(I_{dq0}) \tag{7}$$

$$I_{qs0} = imag(I_{dq0}) \tag{8}$$

Rotor flux linkages in dq0 components:

$$\psi_{a0} = (V_{a0} + R_a \cdot I_{a0}) / \left(i \cdot \omega_{sys_{pu0}}\right) \tag{9}$$

$$\psi_{dqs0} = \psi_{a0} \cdot exp(-i \cdot \theta_{r0}) \tag{10}$$

$$\psi_{ds0} = real(\psi_{dqs0}) \tag{11}$$

$$\psi_{qs0} = imag(\psi_{dqs0}) \tag{12}$$

Rotor field current, voltage, and flux linkage:

$$I_{fd0} = (\psi_{ds0} + L_{du} \cdot I_{ds0}) / L_{md} \tag{13}$$

$$V_{fd0} = R_{fd} \cdot I_{fd0} \tag{14}$$

$$\psi_{fd0} = \beta_{sg} \cdot L_{md} \cdot I_{ds0} + L_{ffdu} \cdot I_{fd0} \tag{15}$$

Where:

S_{set}: Initial power set point

V_{a0}: Phase voltage

I_{a0}: Phase current

R_a: Stator resistance

X_a: Stator inductance

E_{x0}: Effective internal voltage

θ_{r0}: Internal rotor angle

ψ_{a0}: Phase flux linkage

I_{dq0}: Stator direct and quadrature axis current

I_{ds0}: Stator direct axis current

I_{qs0}: Stator quadrature axis current

ψ_{dqs0}: Stator direct and quadrature axis flux linkage

ψ_{ds0} : Stator direct axis flux linkage

ψ_{qs0} : Stator quadrature axis flux linkage

I_{fd0} : Rotor field current

V_{fd0}: Rotor field voltage

L_{du}: Stator unsaturated self-inductance

L_{md}: Direct axis mutual inductance

ψ_{fd0}: Rotor field flux linkage

β_{sg}: Ratio of armature power base to the field power base

L_{ffdu}: Rotor field unsaturated inductance

The initial condition will only be calculated once at the beginning of the simulation, the differential equations that will be used for the rest of the electric machinery simulation will be described in Section IV - B.

IV - A - 2. HYDRAULIC SYSTEM INITIAL CONDITION

Equation (16) through Equation (21) are used to calculate hydraulic system initial conditions [19].

$$P_{shaft} = S_{base} \cdot (P_s + R_a \cdot \left|I_{dq0}\right|^2 + (Drag_m + Drag_{turbine}) \cdot \omega_r \tag{16}$$

$$\tau_{turbine} = P_{shaft}/\omega_{turbine} \tag{17}$$

$$mb = \omega_{turbine} \cdot \frac{Diameter_{turbine}}{2} \cdot A_{gate} \tag{18}$$

$$c = \tau_{turbine} \cdot \frac{A_{gate}}{(Drag_{turbine} \cdot \cos(\theta_{turbine}) + 1) \cdot \rho_{H_2O} \cdot \frac{Diameter_{turbine}}{2}} \tag{19}$$

$$Q_{total} = \frac{\left(mb + \sqrt{mb^2 + 4 \cdot c}\right)}{2} \tag{20}$$

$$P_{water} = \frac{\rho_{H_2O}}{2} \cdot Q_{total}^2 \cdot \left(\frac{1 + Drag_{gate}}{A_{gate}^2} - \frac{1}{A_{pen}^2} \right) \quad (21)$$

Where:

P_{shaft}: Power at shaft （MW）

P_s: Stator power

$Drag_m$: Friction of the machine

$Drag_{turbine}$: Friction of the turbine

ω_r: Turbine angular velocity

$\tau_{turbine}$: Torque at turbine

Q_{total}: Total flow rate (m^3/s)

$\theta_{turbine}$: Angle water leaves the turbine with respect to the entering water, the turbine usually deflect the water axially through about $160°$; the change in momentum provides the torque to drive the runner [18].

ρ_{H_2O}: Density of water ($1000\ g/m^3$)

A_{gate}: Area of gate (m^2)

A_{pen}: Area of penstock (m^2)

P_{water}: Pressure immediately above gate (Pa)

IV - B. ELECTRIC MACHINERY AND HYDRAULIC TRANSIENT MODEL

A detailed electric machinery model consisting of a set of differential equations is used to simulate the electric machinery response during dynamic transients. The MATLAB Ordinary Differential Equations function [20] is used to solve the differential equations. The MATLAB ODE function can solve a given set of first order differential equations with acceptable accuracy and speed. Equation (22) through Equation (35) are the equations used for dynamic electric machinery modeling. Equation (22) through Equation (30) are electrical equations and the Equation (31) through Equation (35) are hydraulic equations. All variables are in per unit unless otherwise stated.

The flux linkages are expressed as:

$$\frac{d\psi_{ds}}{dt} = \omega_{baseE} \cdot \left(V_{sys} \cdot \sin(\gamma_0) + \omega_m \cdot \psi_{qs} + R_a \cdot i_{ds}\right) \tag{22}$$

$$\frac{d\psi_{qs}}{dt} = \omega_{baseE} \cdot \left(V_{sys} \cdot \sin(\gamma_0) + \omega_m \cdot \psi_{ds} + R_a \cdot i_{qs}\right) \tag{23}$$

$$\frac{d\psi_{fd}}{dt} = \omega_{baseE} \cdot \left(V_{fd} - R_{fd} \cdot i_{fd}\right) \tag{24}$$

The rotor and stator transient currents are:

$$pi_{ds} = -L_{du} \cdot i_{ds} + L_{mdu} \cdot i_{fd} - \psi_{ds} \tag{25}$$

$$pi_{qs} = -L_q \cdot i_{qs} - \psi_{qs} \tag{26}$$

$$pi_{fd} = L_{ffdu} \cdot i_{fd} - \beta_{sg} \cdot L_{mdu} \cdot i_{ds} - \psi_{fd} \tag{27}$$

System electric angle and power error equations:

$$\gamma_0 = \left(\omega_m - \omega_{sys}\right) \cdot \omega_{baseE} \tag{28}$$

$$\alpha_{dq} = \omega_{sys} \cdot \omega_{baseE} \tag{29}$$

$$pP_{err} = P_{cmd} - \left(\psi_{ds} \cdot i_{qs} - \psi_{qs} \cdot i_{ds} - \frac{V_{fd} \cdot i_{fd}}{\beta_{fd}}\right) - P_{err} \tag{30}$$

The gate opening, flow rate, and torque of mechanical system:

$$stroke_{fb} = Gain_{ss} \cdot \omega_{corner} \cdot P_{err} \tag{31}$$

$$pQ_{flow} = \left(H_{static} - \frac{P_{water}}{\rho_{H_2O} \cdot g} - \left(\frac{1}{2 \cdot g} + k_{pen}\right) \cdot \left(\frac{Q_{flow}}{A_{pen}}\right)^2\right) \cdot \frac{g \cdot A_{pen}}{L_{pen}} \tag{32}$$

$$pP_{water} = \frac{\rho_{H_2O}}{2} \cdot Q_{flow}^2 \cdot \left(\frac{1 + k_{gate}}{A_n^2} - \frac{1}{A_{pen}^2}\right) - P_{water} \tag{33}$$

$$p\omega_r = \tau_{turbine} - \left(Drag_m + Drag_{turbine}\right) \cdot \omega_r - \left(\psi_{ds} \cdot i_{qs} - \psi_{qs} \cdot i_{ds}\right) \tag{34}$$

$$p\tau_{turbine} = \tau_{turbine} - \left(k_{turbine} \cdot \cos(\theta_{turbine}) + 1\right) \cdot \rho_{H_2O} \cdot Q_{flow} \cdot \frac{d_{turbine}}{2} \cdot \frac{\left(\frac{Q_{flow}}{A_n} - \omega_r \cdot \omega_{baseM} \cdot \frac{d_{turbine}}{2}\right)}{\tau_{base}} \tag{35}$$

Where:

ω_{baseE}: Electrical base angular velocity $2 \cdot \pi \cdot 60\ Hz$

V_{sys}: Power grid voltage

p: Differential operation, equivalent to $\frac{d}{dt}$

Q_{flow}: Volume flow rate (m^3/s)

H_{static}: Static head

P_{water}: Pressure of water in the penstock immediately above the gate $\left(\frac{N}{m^2}\right)$

g: Gravitational acceleration $(9.8\ m/s^2)$

k_{pen}: Penstock loss factor

A_{pen}: Penstock cross sectional area (m^2)

L_{pen}: Penstock length (m)

γ_0: Angle of internal voltage with respect of system voltage

ω_m: Mechanical angular velocity

ω_{sys}: Power system angular velocity

$stroke_{fb}$: Gate stroke feedback

$Gain_{ss}$: Gate open control steady state gain

ω_{corner}: Corner frequency of gate opening controller

k_{gate}: Gate loss factor

$\tau_{turbine}$: Turbine torque

$d_{turbine}$: Diameter of the turbine (m)

α_{dp}: System electrical angle, dq reference frame

A_n: Net open area of the gate

ω_{baseM}: Mechanical angular velocity base

P_{err}: Power error

IV - C. SAMPLE dynamic model simulation result

Figure 11 presents the results for a period of 80 seconds of time to compare the power command and the actual power output. The x-axis is time with units of seconds and the y-axis is power with units of MW. The power command (solid black trace) starts at 80 MW, drops to 40 MW then ramps back to 100 MW. The ramp rate is at the limiting value of 2.5MW/s. The solid red trace is the actual power output of the generator.

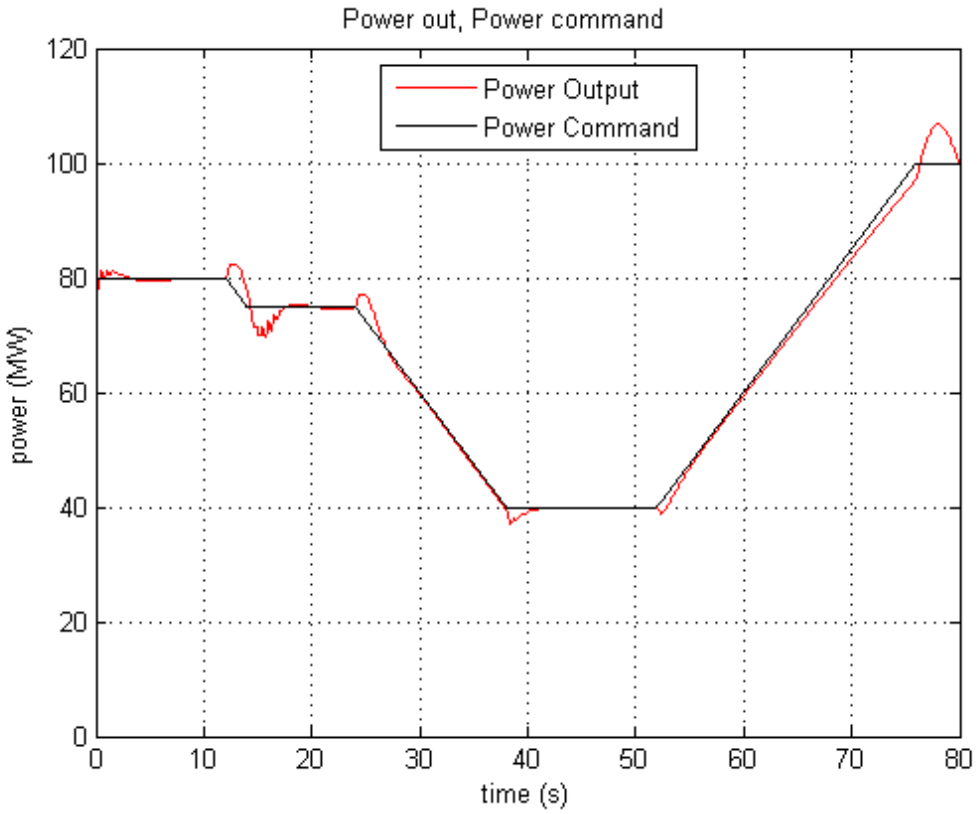

Figure 11 Result of Dynamic Generator Simulation

The plot indicates the generator able to follow the power command at $2.5MW/s$. The efficiency of the penstock combined with the generator is calculated using the ratio of electrical power output over the mechanical power input using the formula:

$$efficiency = \frac{\int P_{out} dt}{\int Q_{flow} dt \cdot \rho_{H_2O} \cdot H_{static}} \tag{36}$$

The efficiency results in 90%. The total energy generated over $80\ s$ is $1.4680\ MW \cdot hr$ and the energy demand is $1.4749\ MW \cdot hr$; the difference is 0.46%. Based on these results, for the purpose analyzing performance over period of years, it is safe to use

ramp function to approximate the power output to improve the simulation run time performance.

It is obvious from Figure 11 that there is transient overshoot opposite to the direction of the set point function change. The cause for that effect is because the water flow does not change immediately due to the inertia of the water; the pressure across the turbine is initially opposite of the change causing the output power to have an opposite direction overshoot [18]. However, while the transient overshoot needs to be looked at closely for penstock transient study, it is not needed for the long term performance study.

IV - D. THE PUMPING MODEL

Based on the generating result it is safe to conclude that the pumped hydro system is able to keep up with the power command closely. Therefore the pump mode behavior is implemented as a ramping function with maximum rate at $2.5MW/s$. This change will decrease the simulation run time significantly. The efficiency of pumping is set at a typical value for large pumps at 87% [19].

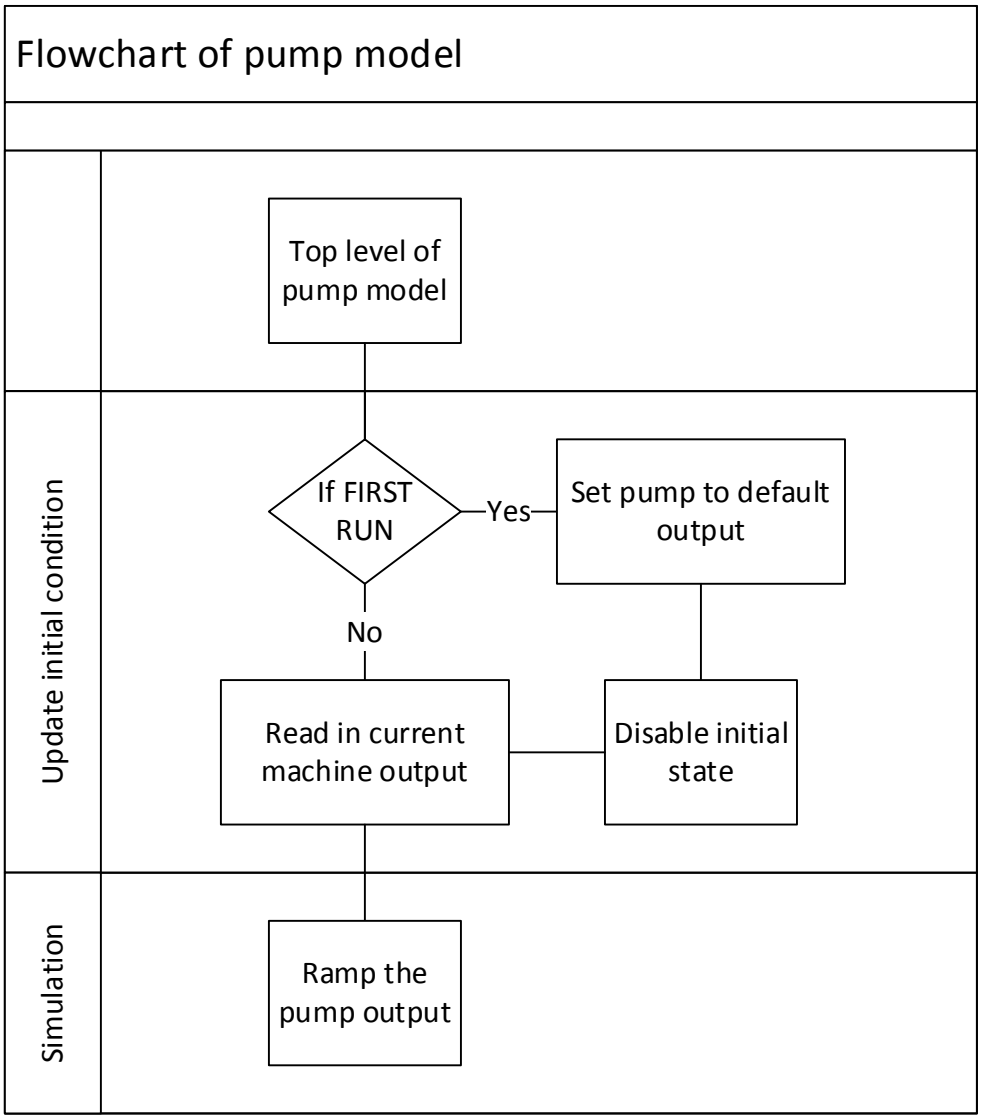

Figure 12 Flowchart of the pump model

The pumping model also has an initial state calculation in the beginning of every pumping simulation. After the initial state has been established, instead of running a series of differential equations, the output value is simply scaled down by the efficiency from the input and then go through a rate limiter to limit the change rate of the output to 2.5 p.u./s, rather than using a full dynamic model for the pumping process.

CHAPTER V. SAMPLE SIMULATION CASE

V - A. SIMULATION SET UP

A simulation was conducted to demonstrate the functionality and the performance of the model. The physical parameters of the hydraulic components are shown in Table 3. The synchronous machine parameters are typical per-unit values from reference [18].

Table 3 Hydraulic components dimension

Penstock		
	Head	$600\ m$
	Cross Sectional Area	$2\ m^2$
	Length	$2100\ m$
	Friction	0.0145
Turbine		
	Turbine Diameter	$3.453\ m$
	Turbine Friction	0.02
	Angle of Water Exit	$15\ °$

The user defines the length of month in units of minutes. Typical month lengths in minutes are listed in Table 4. However in the test simulation case, each month is set to be $60\ minutes$ long, and the total simulation is $48\ months$. This is set to speed up the run time of the model. An actual month contains $43200\ minutes$, which is going to make the simulation much longer; which is less useful for illustration of the model. The actual runtime will be discussed in V - B.

Table 4 List of month length in minutes

1 Day	$1440\ min$
Month with 30 Days	$43200\ min$
Month with 31 Days	$44630\ min$
Month with 28 Days	$40320\ min$
Average length	$43800\ min$

The specified rated generating power for the pumped hydro system is $100\ MW$ and the rated pumping power is $180\ MW$. The rated maximum wind output is $650\ MW$.

V - B. SIMULATION PERFORMANCE

It took $2{,}567.7\ s$, about $42\ min$, to simulate 48 hours of system operation. The time ratio is about $1\ min/1\ hr$, which means every minute of runtime will cover 60 minutes of simulation. For a full year of simulation, it would take will take 6 days to simulate on the platform, assuming there is enough memory for calculation and enough hard drive storage for simulation results. Therefore the simulation process can get tedious and a future optimization method is discussed in Section VI - B - 2. Figure 13 shows the runtime screenshot for the top 5 most time consuming processes in the simulation. The model uses a detailed transient generating model and a simple ramp pumping model. In Figure 13, self time is the time spent in a function excluding time spent in its child functions, and total time is a total time spent in a function including all child functions called. A detailed description of can be found in [21].

Function Name	Calls	Total Time	Self Time*	Total Time Plot (dark band = self time)
UoflCheckAna	1	2567.716 s	15.306 s	
REBP	86402	2549.475 s	9.434 s	
dynamic_gen	86402	2532.532 s	240.502 s	
ode15s	86402	2090.744 s	993.954 s	
funfun\private\daeic12	86402	456.530 s	40.320 s	
DAEqs	3671578	316.926 s	285.798 s	

Figure 13 Simulation rum time break-down

The dynamic gen and it's sub functions took total of 2532.5 s which is only 35 s short of the total simulation time. Of all of its child functions, the process of solving all of the differential equations (ode15s) and algebraic equations (DAEqs) took 1632.313s. It would be more time efficient to set up a full transient model simulating a few seconds' time span and use a ramping model of the generation for long term operation in a future stage of this project. The storage is set to have a $8000\ MW \cdot h$ of capacity which is around $1.29 \cdot 10^9\ Gal$ of water at the height of $600\ m$.

V - C. SIMULATION RESULT

The results of the simulation are shown in Figure 14. The pumping power is the red dashed line. The pump output is zero for most of the time, and the pumping power got maxed out at $180\ MW$ during the windy periods. The generated power is shown in green dashed line. In the plot, it was covered with the blue circles. However the load demand used in our model is zero for the time period we were simulating since the regular generation covered the demand.

The wind power generation is in solid magenta line and it has a rated maximum of $650\ MW$ but the actual wind output has never reached that high during the simulation. The blue circles are CPS2 violations for each $10\ min$ interval, which outputs 1 for a violation and zero for no violation. The violations are using a separate subplot so would be visible. The blue dashed lines are accumulated CPS2 violation count that counts the total number of violation. The CPS2 violations are calculated as described in Section II - A.

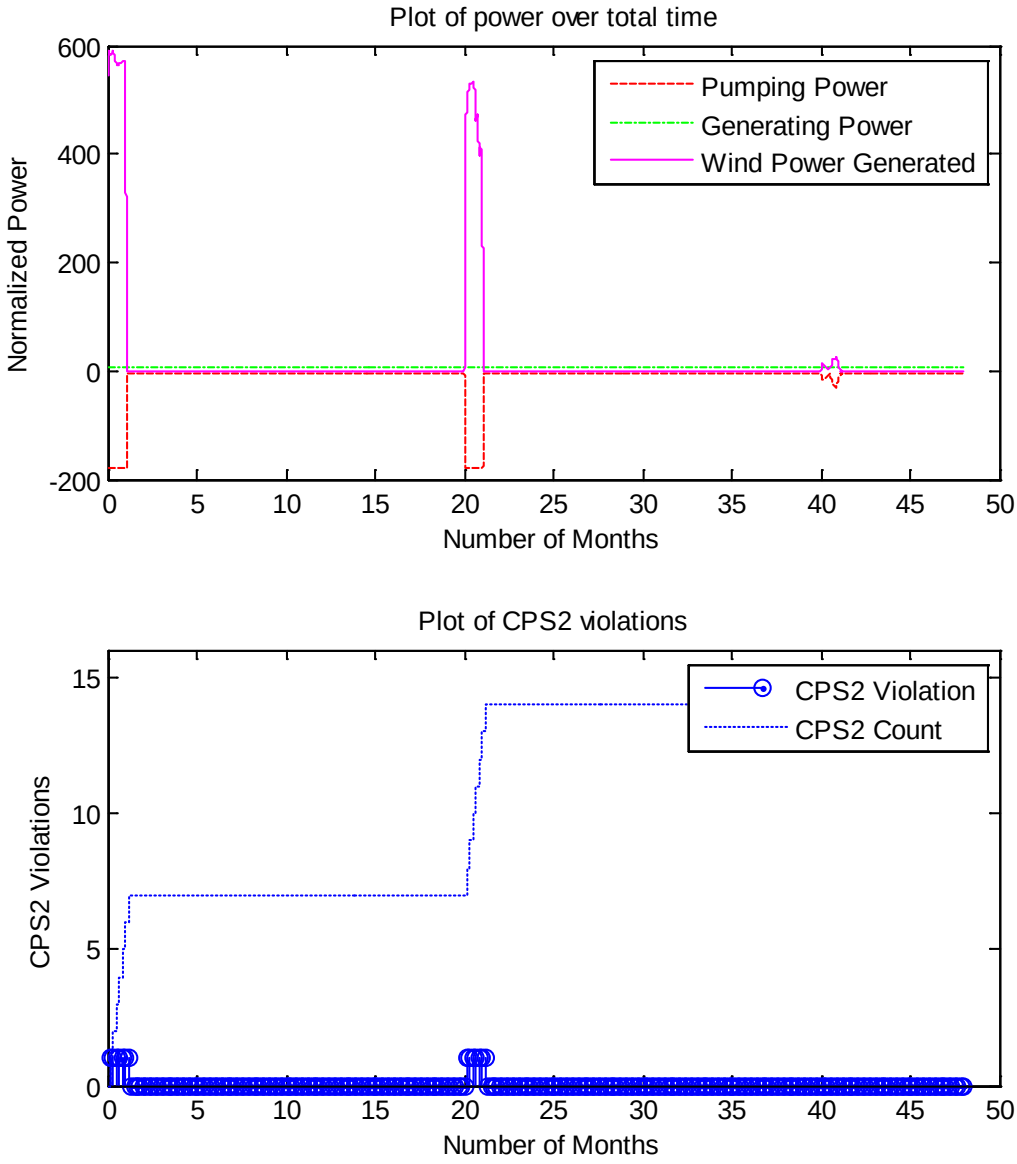

Figure 14 Simulation results for example case

During the simulation, there are a total of 14 CPS2 violations causing 4 CPS2 violation months out of 48 months total. The violations only occur during the "month" when the wind generation exceeds the maximum pumping capacity for more than 10% of the month length in the 1st month and the 20th month. Figure 15 is a zoomed in shot for the pumped hydro operation during the 20th month. There are 7 ten minutes

intervals that received CPS2 violations. As a result, 5 out of 6 intervals in month 20, as well as 2 out of 6 intervals in month 21 resulted in both months being counted as CPS2 violations.

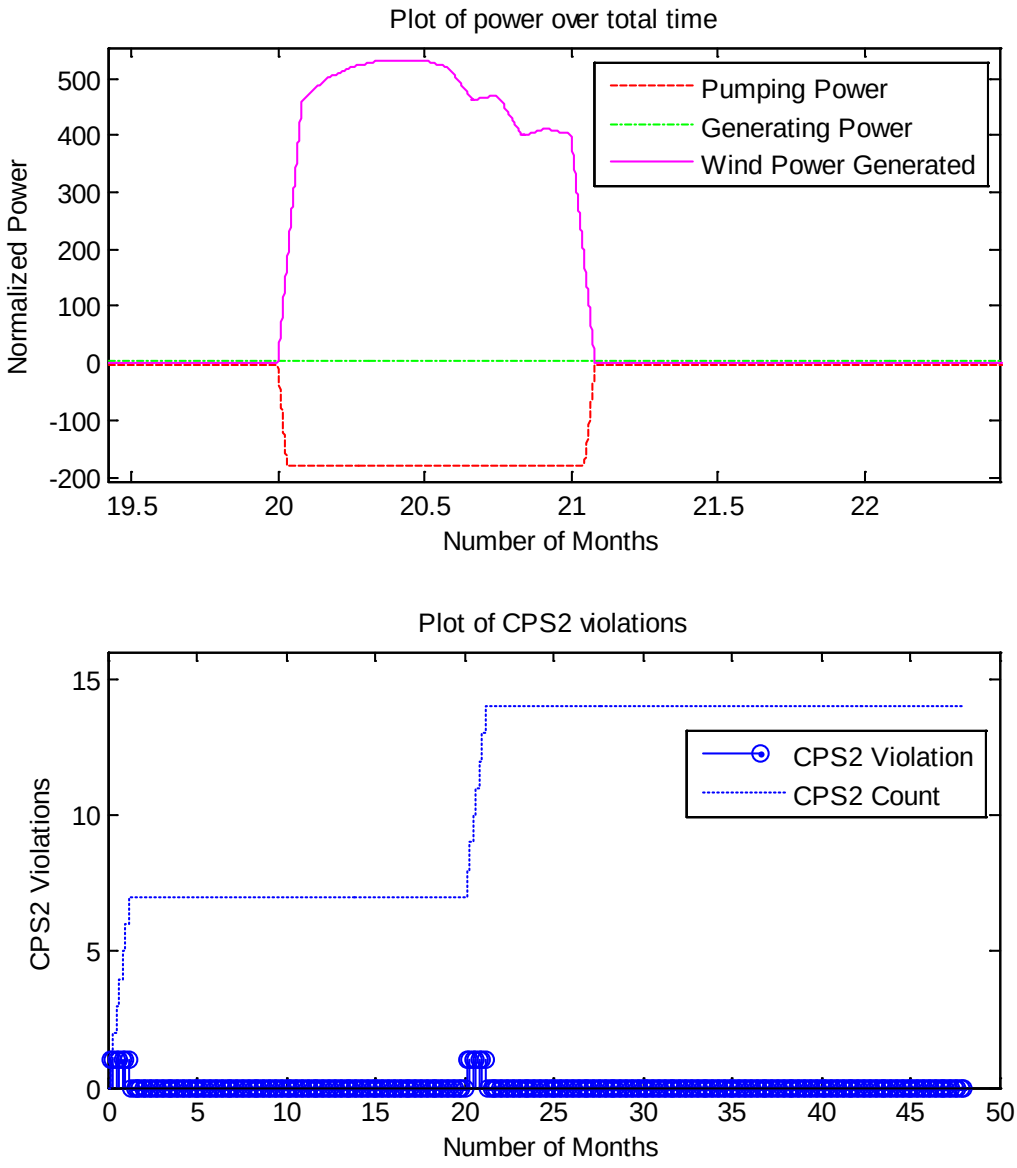

Figure 15 Pumped hydro plant operation during high wind output

It is clear that during month 40 when the wind generation is lower than the rated pump power the pumped hydro was able to completely balance the wind output without setting off any CPS2 violations as shown in Figure 16. The pump input is a mirror image of the wind output. Thus net power error going into the rest of the power system is zero, resulting no frequency deviation violation.

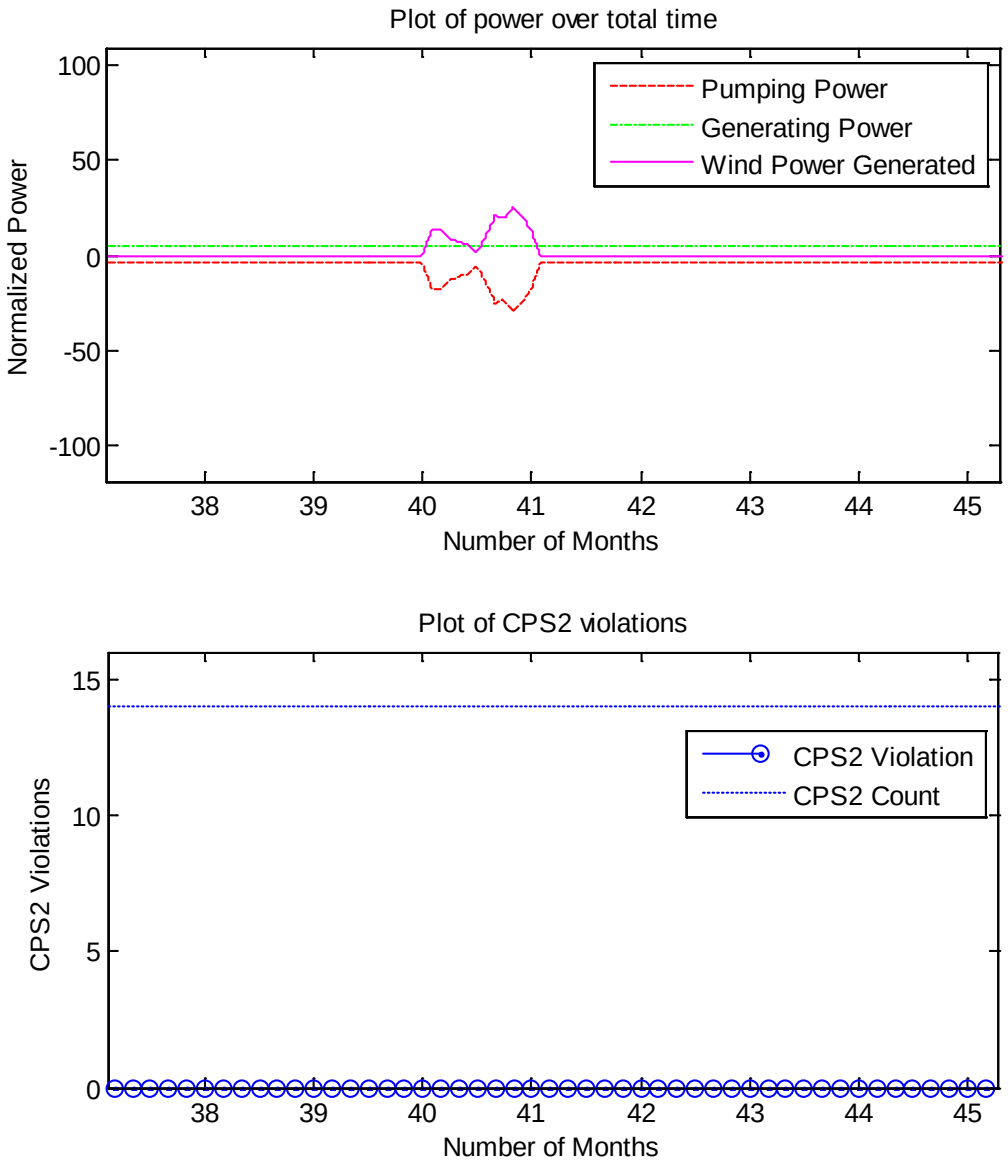

Figure 16 Pumped hydro plant operation during low wind output

In total, there are fourteen 10 min period violations spreading across 4 months of the total 48 months. The final CPS2 score is 92% which exceeds the requirement of 90%.

CHAPTER VI. SUMMARY AND FUTURE WORK

VI - A. SUMMARY

Intermittent renewable energy generation has seen growing penetration over the years as shown in Figure 17 [22]. There has been a steady growth in the non-hydro renewable energy in the United States, in fact, the total renewables percentage had seen a decreasing trend since the 80's until the increase of non-hydro renewables since 2007 [22]. Government policies and falling of the technical barriers have made the intermittent renewable energy more available and affordable than ever.

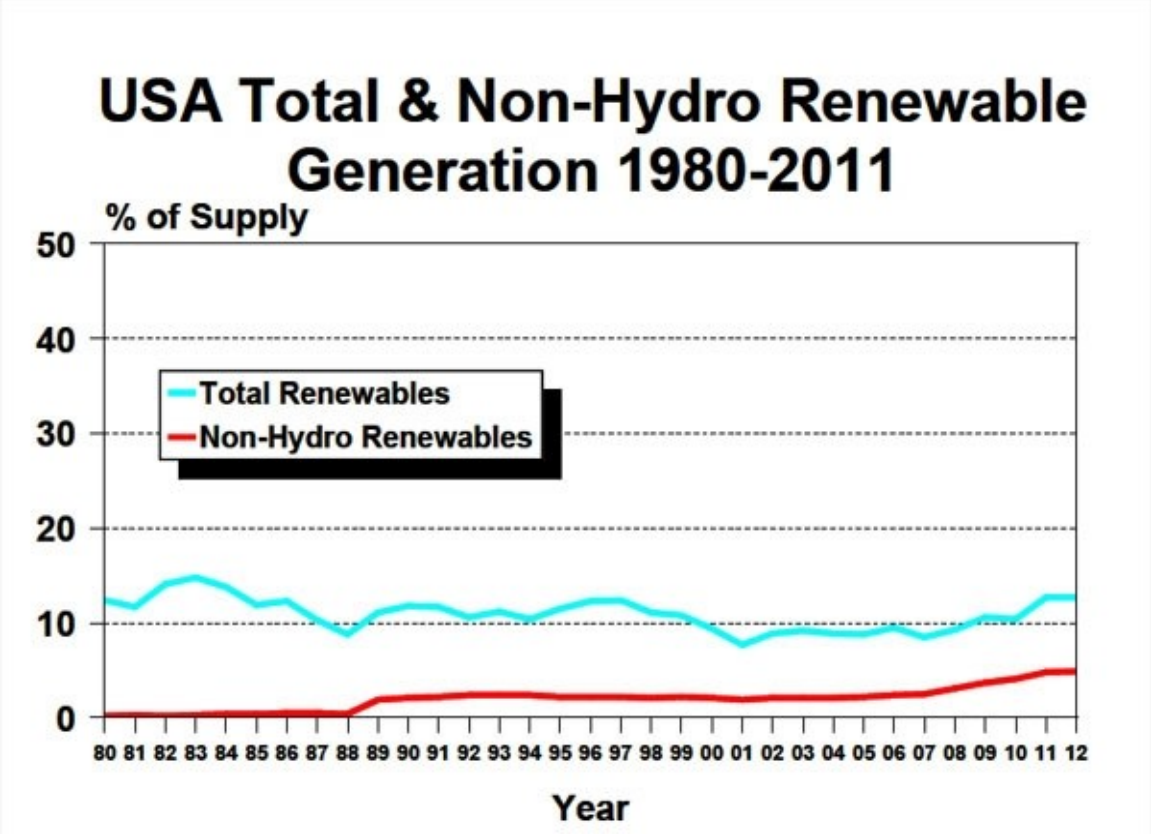

Figure 17 Plot of renewable penetration [22]

Grid storage is needed in order to maintain the increasing intermittent generation penetration with high grid reliability. Of all the grid storage methods discussed in II - B

that are commercially available, pumped hydro plants have the lowest operational cost and excellent cycle efficiency for large bulk energy storage. Traditionally, pumped hydro storage plants require hydroelectric dams which have a fairly large environmental impact. However, newer pumped hydro plants could only require a head water container to be built above an existing body of water, e.g. a river or a lake. Thus, the environmental impact is drastically reduced. The water needed to maintain pumped hydro operation would be minimal once the water container is filled which further reduces the environmental footprint.

Under the crude wind generation and system load estimation use in the sample case, the pumped hydro plant is able to effectively provide the ability to regulate the power system grid frequency with a fast response time. The first order dynamic model used in the simulation provides excellent numerical accuracy, however it lacks the simulation speed for long term self-sustainability study. There is a transient output difference between the detailed model and the steady state ramping model due to transient overshoot in the hydraulic system. A separate transient model can be developed to simulate for a short period of time to determine penstock stability. Nevertheless with the current model setup, the pumped hydro plant is able to operate long term and regulate the grid frequency to meet the CPS2 standard and permit higher intermittent renewable energy penetration into the power system.

VI - B. FUTURE WORK

VI - B - 1. REALISTIC DATA FROM THE WIND GENERATION AND SYSTEM LOAD

The wind generation and the intermittent generation in the simulation example is generated with a random number generator and saved in a data file. It replicated the randomness of the generation but lacked seasonal accuracy as well as grid frequency information. A historical data log that includes intermittent energy output and grid frequency can be used to make the model more realistic and more accurately represent the frequency regulation function of the pumped hydro plant. The system load can also be represented more accurately by using the historical data synchronized to wind data. Traditionally the load can be forecast to an acceptable confidence level and power generation that are fully dispatchable can be used to match the load thus regulate the frequency. The intermittent sources add on another level of variability to the power system supply and demand; in certain scenarios out of forecast load could increase the power mismatch and worsen frequency deviation. In future simulations, a data set, i.e. historical log that closely represent the intermittent renewable generation, power system frequency, and power system load could be used to further study the frequency regulation ability of the pumped hydro storage system.

VI - B - 2. FULL DYNAMIC MODEL WITH SUBTRANSIENT MACHINE MODEL

A full dynamic model with electric machinery subtransient models can be implemented for a component sizing study. It is more computationally efficient to

ignore the transient overshoot while maintaining accuracy during the long term study of the pumped hydro plant using a ramp model as described in IV - C. It would be critical to develop a full transient model, including subtransient response of the synchronous machine for transient study and component sizing for simulations that only cover a few seconds to a few minutes of time span for studying startup and pumping-generating reversal.

VI - B - 3. ELECTRICITY PRICE MODEL

The pumped hydro technology has a competitive price per kilowatt compared to other commercially available grid storage technologies and greater cycle efficiency than most options. Therefore the cost of operation maintenance is relatively low. The pumped hydro storage can not only be used for frequency regulation but also has seen application in load curve shifting and phase shifting. The price of power varies between supply and demand in the power market. The pumped hydro plants should be able to buy power at lower price point and sell power at high price to minimize cost and maximize profit. The price model helps analysis the return cycle of the investment beyond the value from frequency balancing.

REFERENCES

[1] Danish Wind Industry Association, "Guided Tour on Wind Energy," 17 April 2002. [Online]. Available: http://www.windpower.org/tour/index.htm. [Accessed 13 February 2014].

[2] Enerdata, "World Energy Consumption: Map, Figures by Region | 2012," Enerdata, 2013. [Online]. Available: http://yearbook.enerdata.net/electricity-domestic-consumption-data-by-region.html#analyse. [Accessed 13 February 2014].

[3] Observ'ER and Fondation Énergies pour le Monde with the financial support of EDF, "Worldwide electricity production from renewable energy sources," *Fifteenth inventory,* pp. 9-10, 2013.

[4] P. Vennemann, K. H. Gruber, J. U. Haaheim, A. Kunsch, H.-P. Sistenich and H.-R. Thöni, "Pumped Storage Plants - Status and perspectives," *VGB PowerTech,* pp. 32-38, 2011.

[5] J. Painuly, "Barriers to renewable energy penetration; a framework for analysis," *Renewable Energy,* vol. 24, no. 1, pp. 73-89, Sep 2001.

[6] North American Electric Reliability Corporation, "Reliability Standards for the Bulk Electric Systems of North America," 13 May 2009. [Online]. Available:

http://www.nerc.com/docs/standards/rs/Reliability_Standards_Complete_Set.pdf. [Accessed 19 Jun 2012].

[7] North American Electric Reliability Corporation, "Real Power Balancing Control Performance," [Online]. Available: http://www.nerc.com/files/BAL-001-0_1a.pdf. [Accessed 3 June 2013].

[8] North American Electric Reliablity Corporation, "Balancing and frequency control - A technical document prepared by the NERC resources subcommitee," Princeton, NJ, 2011.

[9] I. Gyuk, M. Johnson, J. Vetrano, K. Lynn, W. Parks, R. Handa, L. Kannberg, S. Hearne, K. Waldrip and R. Braccio, "Grid Energy Storage," U.S. Department of Energy, 2013.

[10] Oglethorpe Power, "Types of Power Plants," Oglethorpe Power Corp, 2008. [Online]. Available: http://www.opc.com/PoweringGeorgia/TypesofPowerPlants/index.htm. [Accessed 21 February 2014].

[11] M. Imanaka, Y. Onda, J. Baba, T. Yoshihara and A. Yokoyama, "Feasibility Study on Compensation of Power Fluctuation Caused by Renewable Energy Source Using Desalination System in Island Power System," *Journal of International Council on Electrical Engineering,* vol. 1, no. 3, pp. 345-351, 2011.

[12] Dames and Moore, "National Hydroelectric Power Resources Study, An Assessment of Hydroelectric Pumped Storage, Volume X," The U.S. Army Engineer Institute for water Resources, Washington D.C., 1981.

[13] J. P. Deane, B. P. O Gallachoir and E. J. McKeogh, "Techno-economic review of existing and new pumped hydro energy storage plant," *Renewable and Sustainable Energy Reviews,* vol. 14, pp. 1293-1302, 2010.

[14] B. Roberts, "Capturing Grid Power," *IEEE power & Energy magazine,* vol. 7, no. 4, pp. 32-41, 2009.

[15] U.S. Department of Energy, "Electricity storage can take advantage of daily price variations - Today in Energy - U.S. Energy," U.S. Energy Information Administration, 21 May 2012. [Online]. Available: http://www.eia.gov/todayinenergy/detail.cfm?id=11991. [Accessed 13 SEP 2014].

[16] V. Koritarov, L. Guzowski, J. Feltes, Y. Kazachkov, B. Gong, B. Trouille and P. Donalek, "Modeling Adjustable Speed Pumped Storage Hydro Units Employing Doubly-Fed Induction Machines," Depart of Energy, Oak Rige, TN, 2013.

[17] J. Fenton, "A First Course in Hydraulics," 15 February 2012. [Online]. Available: http://johndfenton.com/Lectures/Hydraulics/Hydraulics.pdf. [Accessed 18 October 2014].

[18] P. Kundar, *Power System Stability and Control*. New York: McGraw-Hill, 1994.

[19] C. T. Crowe, D. F. Elger, B. C. Williams and J. A. Roberson, *Engineering Fluid Mechanics*. John Wiley & Sons, Inc., 2009.

[20] MathWorks, "Ordinary Differential Equations - MATLAB & Simulink," MathWorks, [Online]. Available: http://www.mathworks.com/help/matlab/math/ordinary-differential-equations.html. [Accessed 19 OCT 2014].

[21] "Profiling for Improving Performance - MATLAB & Simulink," The MathWorks, Inc., [Online]. Available: http://www.mathworks.com/help/matlab/matlab_prog/profiling-for-improving-performance.html.

[22] P. Gipe, "Breakdown: Pentration of Renewable Energy in Selected Markets," 17 May 2013. [Online]. Available: http://www.renewableenergyworld.com/rea/news/article/2013/05/penetration-of-renewable-energy-in-selected-markets?page=all. [Accessed 11 November 2014].